Influence of the Line Parameters in Transmission Line Fault Location

Marian Dragomir, Alin Dragomir

Abstract—In the paper, two fault location algorithms are presented for transmission lines which use the line parameters to estimate the distance to the fault. The first algorithm uses only the measurements from one end of the line and the positive and zero sequence parameters of the line, while the second one uses the measurements from both ends of the line and only the positive sequence parameters of the line. The algorithms were tested using a transmission grid transposed in MATLAB. In a first stage it was established a fault location base line, where the algorithms mentioned above estimate the fault locations using the exact line parameters. After that, the positive and zero sequence resistance and reactance of the line were calculated again for different ground resistivity values and then the fault locations were estimated again in order to compare the results with the base line results. The results show that the algorithm which uses the zero sequence impedance of the line is the most sensitive to the line parameters modifications. The other algorithm is less sensitive to the line parameters modification.

Keywords—Estimation algorithms, fault location, line parameters, simulation tool.

I. INTRODUCTION

TRANSMISSION line is one of the most important components of a power system. Due to the fact that these transmission lines cover important areas, they are often exposed to faults. Furthermore, power systems are expanding and along with this expansion stability issues arise in their operation. The use of precise fault location solutions can lead to faster finding of fault and to the minimization of the restoration time of the faulted line. In this way, the stability of the power system and the quality of the energy are fairly improved.

The majority of fault location algorithms use the fundamental frequency phasors of the voltage and current. Another category of the fault location algorithms use the traveling wave components generated by the fault [1], [2]. The fundamental frequency algorithms are cheaper and less complex to implement because they do not need special sensors or high sampling rate equipments. In this case, there can be used the actual sensors and sampling rate equipments (e.g. those used for protection or monitoring) [3]. In some cases, however, there are needed external GPS synchronization sources which increase the implementation cost [4].

The fault location algorithms that use the fundamental frequency phasors of the voltage and current are divided in two main categories: one-end and the two-end data algorithms.

M. Dragomir is with the National Dispatch Center, Bucharest, Romania (e-mail: marian.dragomir@transelectrica.ro).

The one-end data algorithms rely on the estimation of the apparent impedance from the measurement point (e.g. one end of the line) using the voltage and current phasors from the fault regime [5]. In order to obtain the fault location, this apparent impedance is compared with the total impedance of the line. To improve the fault location, some one-end data fault location algorithms are used in addition the pre-fault voltage and current phasors [6]. The one-end data algorithms are cheap and very simple to implement, which is why the fault location using one-ended voltage and current phasors has became a standard feature in the majority of the numerical relays [4]. In the other hand, the precision of these algorithms is affected by many source of errors such as: value of the fault resistance, the remote in-fed current, value of the zero-sequence line impedance, errors in current phasor estimation due to the decaying DC component from the fault current [3]-[7].

The two-end data algorithms estimate the fault location using the measurements from both ends of the line. In the standard approach, these measurements contain the voltage and current phasors from both ends of the line [8], but over the past years there were developed two-end data algorithms which use only the current phasors [9] or only the voltage phasors [10]. The two-end data algorithms can use synchronized or unsynchronized measurements. The two-ended synchronized measurements need an external GPS source which increases the cost of implementation, but on the other hand, it increases the fault location precision [1], [9]. The two-ended unsynchronized algorithms can be used where synchronized timing is too expensive. In order to obtain as precise results as possible, the goal of the unsynchronized algorithms is to synchronize the measurements off-line. The off-line synchronization can be done manually or using dedicated software [11].

In order to estimate the fault location, the power frequency phasor algorithms need the positive sequence, and in some cases, the zero sequence values of the line impedance. Taking into account that these impedance values may vary with the ground resistivity and with the ambient temperature, it is useful to analyze their influence in fault location estimation.

The paper focuses on the influence of the ground resistivity in positive and zero sequence impedance values, and furthermore, in fault location estimation.

II. VARIATION OF THE LINE PARAMETERS

The parameters of the line are calculated in most cases using the tower configuration and the properties of the conductor material [12], [13]. In some special cases, if the line

parameters need to be accurately known there are conducted field tests which require the outage of the line. In both cases, the resulted values of the positive and zero sequence line impedance are implemented in the relay that protects the line and are also used in fault location estimation process.

In real operation conditions these parameters may vary and along with this variation may appear problems in distance protection operation and fault location estimation.

In order to see how these parameters vary, first there is used a line constants program to determine the line parameters of a typical power transmission line which has the tower configuration, as depicted in Fig. 1.
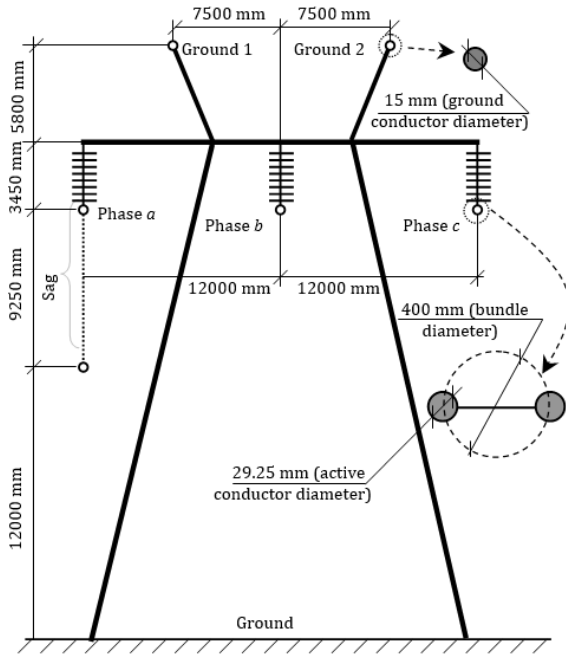

Fig. 1 Tower configuration of a typical power transmission line

TABLE I
LINE PARAMETERS AT 20°C

Positive Sequence		Zero Sequence	
R_1 (Ω/km)	X_1 (Ω/km)	R_0 (Ω/km)	X_0 (Ω/km)
0.0169	0.2722	0.2633	0.9741

Each phase bundle contains two ACSR (aluminum conductor steel-reinforced) active conductors 450 mm^2 each. Taking into account that the ground resistivity, ρ, used to compute the line parameters is 100 Ω·m, in Table I there are shown the positive and zero sequence values of the line resistance, R, and reactance, X, at 20°C.

For a single circuit line the parameters are affected by several factors, including the ambient temperature and the ground resistivity. For example, the resistance varies with the ambient temperature in a linear fashion [14], as in Fig. 2, where R is the resistance calculated at different temperature values and $R_{20°C}$ is the resistance at 20°C. In Fig. 3 there is illustrated the variation of the line parameters with ground resistivity, where R_1 and X_1 are the positive sequence

resistance and reactance of the line calculated for different ground resistivities, R_{1_100} and X_{1_100} are the positive sequence resistance and reactance of the line calculated for the ground resistivity reference value of 100 Ω·m, R_0 and X_0 are the zero sequence resistance and reactance of the line calculated for different ground resistivities, R_{0_100} and X_{0_100} are the zero sequence resistance and reactance of the line calculated for the ground resistivity reference value of 100 Ω·m. All the parameters mentioned above are calculated using the tower configuration depicted in Fig. 1.
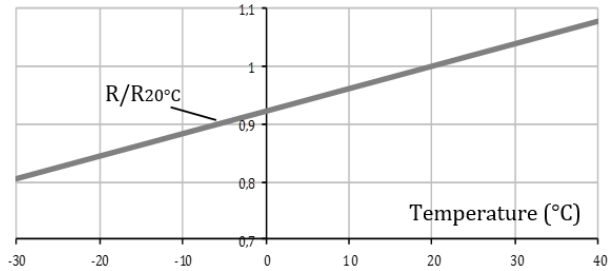

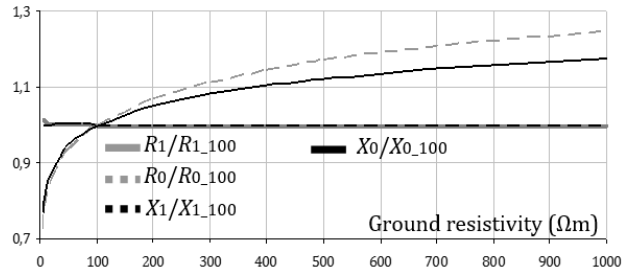Fig. 2 Dependence of the resistance with temperature

Fig. 3 Dependence of the line parameters with ground resistivity

As it can be seen from Fig. 3, the positive sequence parameters are practically not affected by the modification of the ground resistivity. On the other hand, the zero sequence parameters are strongly affected by the modification of ground resistivity. From Fig. 3 it can be observed that for the zero sequence resistance, R_0, the variation becomes pithier for ground resistivity values greater than 200 Ω·m when compared with the zero sequence reactance, X_0.

III. FAULT LOCATION ALGORITHMS

A. One-End Data Algorithms

The majority of the transmission lines are equipped with numerical relays, where the one-ended fault location function is implemented. To illustrate how the fault location is calculated, first it is considered a three-phase line connected to sources which experience a fault in point **F** on phase *a*, like in Fig. 4, where the variables are as follow: $\underline{E}_{Sa}$, $\underline{E}_{Sb}$ and $\underline{E}_{Sc}$ are the source **S** voltage phasors, $\underline{E}_{Ra}$, $\underline{E}_{Rb}$ and $\underline{E}_{Rc}$ are the source **R** voltage phasors, $\underline{I}_{Sa}$, $\underline{I}_{Sb}$ and $\underline{I}_{Sc}$ are the current phasors measured at end **S**, $\underline{V}_{Sa}$ is the voltage phasor measured at end **S**, $\underline{Z}_{La}$, $\underline{Z}_{Lb}$ and $\underline{Z}_{Lc}$ are the line self-impedances corresponding to phase *a*, phase *b* and phase *c*, R_F is the fault resistance, $\underline{Z}_m$ is

the mutual impedance which is considered equal between the phases, $\underline{I}_{Ra}$ is the remote current phasor on phase a, $\underline{I}_F$ is the fault current and d is the per-unit distance to the fault measured from end **S** of the line.

The phase a voltage measured at end **S** of the line is:

$$\underline{V}_{Sa} = d\,(\underline{Z}_{La}\,\underline{I}_{Sa} + \underline{Z}_m\,\underline{I}_{Sb} + \underline{Z}_m\,\underline{I}_{Sc}) + R_F\,\underline{I}_F \qquad (1)$$

where $\underline{I}_F = \underline{I}_{Sa} + \underline{I}_{Ra}$. Using the measured phase currents at end **S,** it can be calculated the zero sequence current $\underline{I}_{S0}$ as follows:

$$\underline{I}_{S0} = \underline{I}_{Sa} + \underline{I}_{Sb} + \underline{I}_{Sc} \qquad (2)$$

If (2) is introduced in (1), it can be obtained as:

$$\underline{V}_{Sa} = d[\underline{Z}_{La}\,\underline{I}_{Sa} + \underline{Z}_m\,(\underline{I}_{S0} - \underline{I}_{Sa})] + R_F\,(\underline{I}_{Sa} + \underline{I}_{Ra}) \qquad (3)$$
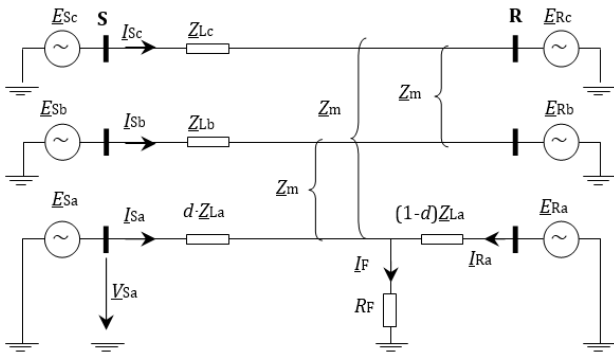

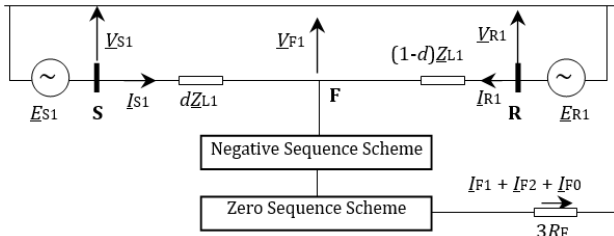Fig. 4 Simple two-sources grid with fault on phase a

Fig. 5 Sequence schemes connection for phase a-to-ground fault

The phase a line self-impedance $\underline{Z}_{La}$ and the mutual impedance $\underline{Z}_m$ can be calculated using the line's positive sequence impedance $\underline{Z}_{L1}$ and the zero sequence impedance $\underline{Z}_{L0}$, as:

$$\underline{Z}_{La} = (\underline{Z}_{L0} + 2\underline{Z}_{L1})/3 \; , \; \underline{Z}_m = (\underline{Z}_{L0} - \underline{Z}_{L1})/3 \qquad (4)$$

Replacing $\underline{Z}_{La}$ and $\underline{Z}_m$ calculated with (4) in (3) and making simple mathematical operations it results in:

$$\underline{V}_{Sa} = d\,\underline{Z}_{L1}(\underline{I}_{Sa} + \underline{k}_0\,\underline{I}_{S0}) + R_F\,(\underline{I}_{Sa} + \underline{I}_{Ra}) \qquad (5)$$

with $\underline{k}_0 = (\underline{Z}_{L0} - \underline{Z}_{L1})/(3\cdot\underline{Z}_{L1})$ being the compensation factor. The current phasors of the faulted phase can be divided in pre-fault and pure fault components as in (6):

$$\underline{I}_{Sa} = \underline{I}_{Sa\_PRE} + \underline{I}_{Sa\_F} \,, \; \underline{I}_{Ra} = \underline{I}_{Ra\_PRE} + \underline{I}_{Ra\_F} \qquad (6)$$

where the subscript "PRE" denotes the pre-fault component and the subscript "F" denotes the pure fault component. Supposing that $\underline{I} = \underline{I}_{Sa} + \underline{k}_0\cdot\underline{I}_{S0}$, (5) results in:

$$\underline{V}_{Sa} = d\,\underline{Z}_{L1}\,\underline{I} + R_F\,(\underline{I}_{Sa} + \underline{I}_{Ra}) \qquad (7)$$

Replacing (6) in (7) and extracting the fault resistance R_F, results in:

$$R_F = (\underline{V}_{Sa} - d\,\underline{Z}_{L1}\,\underline{I})/[\underline{I}_{Sa\_F}(1 + \underline{I}_{Ra\_F}/\underline{I}_{Sa\_F})] \qquad (8)$$

Supposing that $\underline{I}_{Sa\_F}$ is in phase with $\underline{I}_{Ra\_F}$ and extracting the imaginary part of (8) will result in:

$$\mathrm{Im}\{(\underline{V}_{Sa} - d\,\underline{Z}_{L1}\,\underline{I})/\underline{I}_{Sa\_F}\} = 0 \qquad (9)$$

and extracting the per-unit distance to the fault location measured from end **S** of the line, d, will result in:

$$d = \mathrm{Im}\{\underline{V}_{Sa}\,\underline{I}_{Sa\_F}^{*}\}/\mathrm{Im}\{\underline{Z}_{L1}\,\underline{I}\underline{I}_{Sa\_F}^{*}\} \qquad (10)$$

where the superscript "*" denotes the complex conjugate and $\underline{I}_{Sa\_F}$ is obtained with (6). Equation (10) represents the fundamental fault location equation using one-ended voltage and current phasor measurements [6].

B. Two-End Data Algorithms

For power transmission lines where the synchronized voltage and current phasors can be obtained from both ends of the line, a two-end data fault location algorithm can be applied [8]. The principle of this algorithm is that the voltage along the line can be represented as a function of the distance to the fault point, d. Considering the same faulted grid as in Figs. 4 and 5 there is presented the connection of the sequence schemes for a phase-to-ground fault in point **F**. The variables from Fig. 5 are as follows: $\underline{V}_{S1}$ and $\underline{V}_{R1}$ are the positive sequence voltage phasors at end **S** and **R**, $\underline{I}_{S1}$ and $\underline{I}_{R1}$ are the positive sequence current phasors at end **S** and **R**, $\underline{V}_{F1}$ is the positive sequence voltage at the fault point, $\underline{I}_{F1}$, $\underline{I}_{F2}$ and $\underline{I}_{F0}$ are the positive, negative and zero sequence currents at the fault point. The positive sequence voltage at the fault point $\underline{V}_{F1}$, seen from end **S** and from end **R**, is calculated with (11) and (12):

$$\underline{V}_{F1} = \underline{V}_{S1} - d\,\underline{Z}_{L1}\,\underline{I}_{S1} \qquad (11)$$

$$\underline{V}_{F1} = \underline{V}_{R1} - (1 - d)\underline{Z}_{L1}\,\underline{I}_{R1} \qquad (12)$$

Equating (11) and (12) and solving for d results in:

$$d = (\underline{V}_{S1} - \underline{V}_{R1} + \underline{Z}_{L1}\,\underline{I}_{R1})/(\underline{Z}_{L1}\,\underline{I}_{R1} + \underline{Z}_{L1}\,\underline{I}_{S1}) \qquad (13)$$

The advantage of this technique is that it does not need the fault type to estimate the fault location.

IV. SIMULATION RESULTS AND COMMENTS

The simulation results reveal the influence of the ground resistivity in line parameters estimation and further more in fault location estimation of the algorithms presented in the previous section.

In a first stage, it was used the line constants program incorporated in MATLAB environment to calculate the parameters of a line using the tower configuration depicted in Fig. 1 and the ground resistivity value of 100 $\Omega \cdot$m (see Table I). These parameters were implemented in the line blocks of the MATLAB simulation model of the grid depicted in Fig. 6. The grid's nominal frequency is 50 Hz, while the nominal voltage is 400 kV. The total length of the line L is 100 km, the end **S** short-circuit power S_{SC_S} is 3000 MVA and the end **R** short-circuit power S_{SC_R} is 1000 MVA. There were simulated single-phase-to-ground faults, taking into account that the value of the fault resistance, R_F, is 10^{-6} Ω and the difference between the sources' angles is 0°. With all these in mind, the faults were simulated every 10 km along the line, starting with end **S** of the line. For each case, the fault location was calculated with the algorithms depicted in Section III.
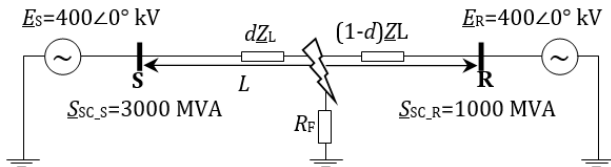
E_S=400∠0° kV $\qquad$ E_R=400∠0° kV

dZ_L $\quad$ $(1-d)Z_L$

S $\qquad$ **R**

L

S_{SC_S}=3000 MVA $\qquad$ S_{SC_R}=1000 MVA

R_F

Fig. 6 One-line scheme of the test grid implemented in MATLAB

TABLE II
DIFFERENT SOIL TYPES

Type of soil	Ground resistivity ($\Omega \cdot$m)
Wet loam	20
Chernozem	50
Clay, argil	80
Loess	200
Sandy soil	300

The results obtained represent the base results and they will be used as reference for the fault location estimations when line parameters are estimated for different values of the ground resistivity.

In a second stage there were considered different soil types which have the ground resistivity values, as depicted in Table II. For each type of soil there were computed again the line parameters using the same tower configuration and the values were implemented in the line blocks of the test grid and then the single-phase-to-ground faults were simulated again in the same locations. Note that when the fault locations were computed with the same algorithms, the input data referring to the line parameters remain the one estimated for the ground resistivity value of 100 $\Omega \cdot$m. The errors in fault location estimation for the one-end data algorithm are shown in Fig. 7, while the results for the two-end data algorithm are shown in Fig. 8. The errors in (%) were calculated with (14), where d_{100} represent the fault location computed for the ground resistivity value of 100 $\Omega \cdot$m and d is the fault location computed for
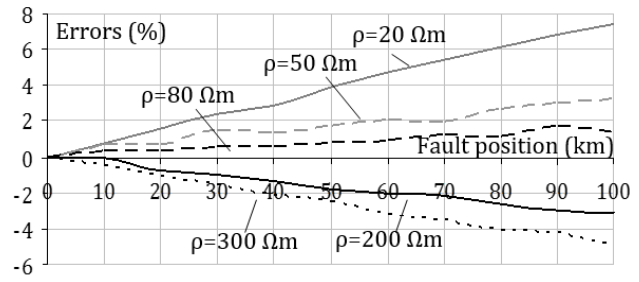
different ground resistivity values.
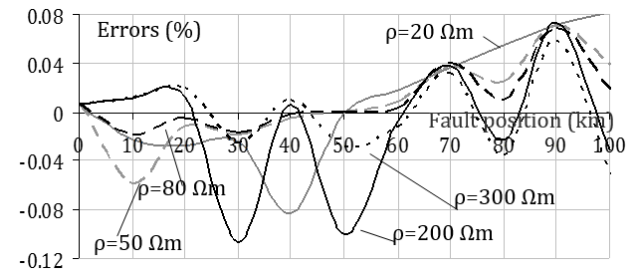

Fig. 7 Errors introduced by the one-end data algorithm

Fig. 8 Errors introduced by the two-end data algorithm

$$Error = (d_{100} - d) \cdot 100 \qquad (14)$$

As it can be seen, the one-end data algorithm is strongly affected by the variation of the line parameters due to the modification of the ground resistivity and the errors in fault location increase with the increase of the distance between the fault point and end **S** of the line. This is due to the fact that the algorithm uses both the positive and zero sequence parameters of the line which are strongly affected by the variation of the ground resistivity (see Fig. 3). The two-end data algorithm is much less affected by the variation of the line parameters, irrespective with the fault position along the line. This is due to the fact that the algorithm uses only the positive sequence parameters of the line.

Taking into account that the power transmission lines cross areas with different soil types, for those lines equipped with one-end data fault locators it is useful to reconsider the zero sequence impedance components in order to minimize the fault location errors. This can be done by calculating the zero sequence impedance for line portions which cross certain soil types and then obtain the total value of the zero sequence line impedance by summing all values obtained above.

REFERENCES

[1] M. M. Saha, J. J. Izykowski, and E. Rosolowski, *Fault location on power networks*, London: Springer, 2010, ch. 6.
[2] *IEEE Guide for determining fault location on AC transmission and distribution lines*, IEEE C37.114 Standard.
[3] E. O. Schweitzer III, *A review of impedance-based fault locating experience*, 14th Annual Iowa-Nebraska System Protection Seminar, October 1990.
[4] K. Zimmerman and D. Costello, *Impedance-based fault location experience*, Proceedings of the 58th Annual Conference for Protective Relay Engineers, April, 2005, pp. 211 – 226.

[5] S. Das and S. Santoso, *Impedance-based fault location in transmission networks: theory and application*, IEEE Access, Vol. 2, June 2014, pp. 537-557.

[6] T. Takagi and Y. Yamakoshi, *Development of a new type fault locator using the one-terminal voltage and current data*, IEEE Transactions on Power Apparatus and Systems, Vol. PAS-101, No. 8, 1982, pp. 2892-2898.

[7] L. Eriksson, M.M. Saha and G.D. Rockefeller, *An accurate fault locator with compensation for apparent reactance in the fault resistance resulting from remote-end infeed*, IEEE Transactions on Power Apparatus and Systems, Vol. PAS-104, No. 2, 1985, pp. 424-436.

[8] K. P. Lien, *A novel fault location algorithm for multi-terminal lines using phasor measurement unit*. Proceedings of the 37th Annual North American Power Symposium; October 2005; pp. 576–581.

[9] O. Avendano, *Tutorial on fault locating embedded in line current differential relays – methods, implementation, and application considerations*, 17th Annual Georgia Tech Fault and Disturbance Analysis Conference, April 2014.

[10] M. Istrate, *Single-phased fault location on transmission lines using unsynchronized voltages*, Advances in Electrical and Computer Engineering, Vol 9, Issue 3, 2009.

[11] D. Spoor and K. Hinley, *Unsynchronised fault location on asymmetrical lines*, CIGRE, South East Asia Protection and Automation Conference, 17-18 March, 2015.

[12] H. E. Prado-Félix, V. H. Serna-Reyna, M. V. Mynam, M. Donolo and A. Guzmán, *Improve Transmission Fault Location and Distance Protection Using Accurate Line Parameters*, 17th Annual Georgia Tech Fault and Disturbance Analysis Conference, April 2014.

[13] A. Amberg, A. Rangel, and G. Smelich, *Validating Transmission Line Impedances Using Known Event Data*, Proceedings of the 65th Annual Conference for Protective Relay Engineers, April 2012.

[14] M. Bockarjova and G. Andersson, *Transmission Line Conductor Temperature Impact on State Estimation Accuracy*, Proceedings of IEEE POWERTECH Conference, 1-5 July, 2007, Lausanne, Switzerland, pp. 701-706.

Marian Dragomir received the bachelor degree in electrical engineering from "Gheorghe Asachi" Technical University of Iasi, Romania, in 2008 and the Ph.D degree in electrical engineering from the same institution in 2011. From 2011 he is with the National Dispatch Center, Bucharest, Romania.